Proceedings of the
Annual Stability Conference
Structural Stability Research Council
Charlotte, North Carolina, April 11-14, 2022

Composite timber veneer-wrapped steel columns – proof of concept through tests and numerical simulations

Valentino Vigneri[1], Andreas Taras[2]

Abstract
The qualities of timber as an environmentally friendly building material are increasingly being recognized, as its use may lead to several advantages, such as renewability and carbon sequestration. However, timber presents a number of inherent disadvantages in terms of structural performance, such as its reduced ductility and the comparative lack of strength which affects the sizing of structural elements. This is only partly addressed by the development of standardized wood-derived products, since the long-term deterioration of the mechanical properties may undermine the robustness and durability of the system. In order to overcome these issues, composite systems that combine steel with timber can represent a structurally effective solution, while promoting the use of both materials in construction. This paper presents a newly conceived steel-timber composite column consisting of a steel hollow section wrapped in various layers of veneer lumber. Whilst the use of structural steel allows the reduction of the dimensions of the cross-section compared to a pure timber column, the multiple outer veneer-lumber layers stabilize the inner thin-walled steel profile by restricting cross-sectional deformation and hindering potential local as well as global buckling. The planned experimental campaign and the fabrication process of the specimens are detailed in the paper while the results of preliminary numerical simulations are presented and discussed. The work was conducted in the frame of an applied research project to evaluate the potential of the proposed solution and it represents a contribution toward the development of hybrid structural solutions, maintaining steel construction at its core.

1. Introduction

Nowadays, the advantages of timber as a more sustainable construction material have become more and more relevant and many recent structural applications involving its use can be increasingly found all over the globe. In parallel, the research in the field of timber structures proceeds quickly along with the standardization of an increasing number of engineering wood products. However, due to its relatively modest strength, together with the well-known inherent durability issues, timber elements are often employed in combination with other materials. Several recent studies promoting this approach in practice can be found in literature, where timber has

[1] Postdoctoral researcher, Steel and Composite Structures, ETH Zürich, <vigneri@ibk.baug.ethz.ch>
[2] Full professor, Chair of Steel and Composite Structures, ETH Zürich, <taras@ ibk.baug.ethz.ch>

been combined with steel (Hassanieh, Valipour, & Bradford, 2016; Loss, Piazza, & Zandonini, 2016; Romero, Yang, Hanus, & Odenbreit, 2022) and concrete (Shan, Xiao, Zhang, & Liu, 2017; Djoubissie, Messan, Fournely, & Bouchaïr, 2018; Fragiacomo, 2013; Oudjene, et al., 2018; Zhu, et al., 2019), and in hybrid column-beam systems (Karagiannis, Málaga-Chuquitaype, & Elghazouli, 2017).

Among the different composite solutions currently available on the market, a good combination of steel and timber elements can lead to high-performance structural elements with reduced dimensions and weight. This aspect is particularly important in the case of columns, where the use of only timber columns in multi-story buildings may result in large cross-section dimensions of the columns. Nevertheless, only a few recent studies focused on composite steel-timber columns are available and a vast majority of them concerned timber-infilled steel profiles (Ghanbari-Ghazijahani, Magsi, Gu, Nabati, & Ng, 2019; Karampour, et al., 2020).

An alternative approach for increasing the stability of hollow steel profiles can be jacketed through an outer concrete-infilled tube and/or using CFRP strips. As confirmed by several studies, the confinement effect of the outer layers onto the steel tube results in a significant increase in the buckling resistance as well as in its ductility. (Liang, Uy, & Liew, 2006; Karimi, El-Dakhakhni, & Tait, 2011; Karimi, K; Tait, M J; El-Dakhakhni, W. W., 2011).

Only two recent studies investigated the behavior of composite steel-timber columns made of an inner structural steel element embedded in timber. Specifically, Hu et al. (2020) presented a HEA steel profile encased and fixed to a slotted and milled glued laminated timber element using epoxy adhesive, as shown in Figure 1. Composite steel-timber as well as steel and timber specimens were tested separately for three different lengths. Among the results presented, it was shown experimentally that the combination of steel-timber composite columns leads to a resistance slightly higher than the superposition of the single elements (steel + timber) in some cases. This outcome shows that an efficient combination of steel and timber can overcome the benefits of the individual materials. Subsequently, Kia and Valipour (2021) published another experimental study where steel profiles were embedded in timber. It was found that the use of embedded high-strength steel bars increases the strength-to-weight ratio up to +81% compared to the respective timber column. Furthermore, it was observed that the increase in the resistance given by the timber is inversely proportional to its compressive strength. However, this aspect seems to be related to the lower crushing strain which favors a more effective composite action as the yield strain of steel is much lower in consideration of the cross-sectional strain compatibility.

2. Motivation

Whilst recent research developments in composite steel-timber floor systems have shown promising results, only little attention has been given to columns, as confirmed by the scientific literature available. Along with the widespread use of high-strength structural steel in the last years, more slender geometries have become possible, while allowing for greater material savings. However, these columns typically undergo global flexural (and local) buckling which prevents the exploitation of the full plastic resistance. Although this issue can be surely tackled by combining steel profiles and timber elements in an effective manner, further investigations are essential to find out the optimal compromise between materials and mechanical performance.

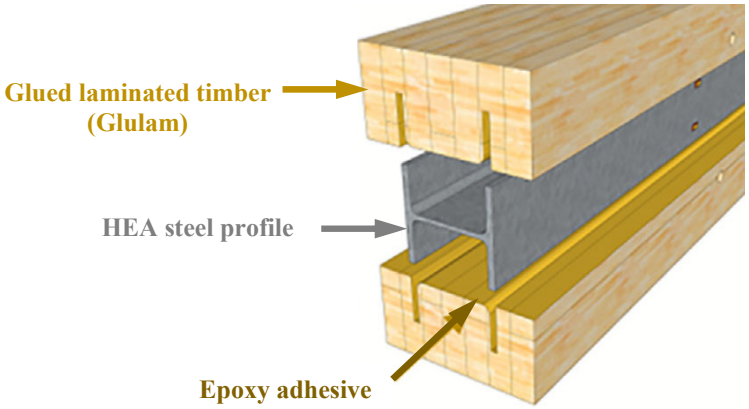

Figure 1: HEA Steel profile embedded in Glulam timber and tested by Hu et al. (2020)

Therefore, a newly conceived timber veneer-wrapped steel column is proposed in this contribution consisting of a hollow circular steel profile wrapped by several veneer sheets which provide confinement to the inner core while increasing the buckling resistance. However, the main objectives of this work lie not only in the enhancement of the mechanical performance of the column, providing a valid alternative to more conventional solutions but also in the fabrication process which represents a fundamental step in the development of a new structural product. The concept behind the newly conceived composite column is explained in Section 3, and the aforementioned objectives are tackled through an experimental campaign presented in Section 4, and by means of a preliminary numerical study described and discussed in Section 5, before drawing the main conclusions in Section 6.

3. Concept

The presented steel-veneer columns, named “STIMBER-COL”, consist of an inner high-strength steel hollow section wrapped by multiple thin timber-veneer layers which increases significantly the stability of the composite member. The cross-section of the inner profile may be either circular or squared but the presented study focuses only on the former geometry. Unlike engineering timber materials such as laminated veneer lumber (LVL) or “Glulam”, a key feature of veneer lies in the reduced thickness (between 0.5 and 1 mm) which guarantees a certain degree of flexibility and workability. This facilitates the placement as well as the gluing of the veneer sheets onto the curved steel surface over its perimeter enabling an adequate bond between the materials. A slight inclination with respect to the longitudinal direction could be also applied to the veneer sheets prior to their application to stiffen the resulting outer tube along the circumferential direction, so increasing the confinement effect. The main concept of the proposed “STIMBER-COL” is finally summarized in Figure 2.

Figure 2: Concept of STIMBER-COL

The composite column is expected to deliver high performance, reaching elevated resistances thanks to the high-strength steel tube and the stabilization provided by the outer timber veneer tube.

From preliminary analytical calculations, a standard 3 m "STIMBER-COL" column with an outer diameter of 150 mm is expected to withstand vertical loads of over 500 kN and it could therefore potentially become a valid and slenderer alternative to timber columns and reinforced concrete columns. Besides the thermal protection of the outer veneer layers on the inner high-strength steel tube, the technology also provides high impact resistance of the column, which could be useful in some building applications.

Despite the promising perspective in terms of structural performance, the fabrication represents a crucial aspect which needs to be properly addressed and thus, it is discussed in the next section.

4. Planned experimental study

4.1. Fabrication of the specimens

In the planned experimental study, the fabrication of the specimens is not only the first and foremost step prior to testing, but it is crucial for assessing the feasibility of such an unconventional steel-timber column. For this purpose, a special fabrication procedure is developed and described in this section while the flow-chart in Figure 3 summarizes the steps. Although this approach shares some similarities with the production process of the patented tubes "LIGNOTUBE" (LIGNOTUBE, 2023), these are suitable for non-structural applications and the length is fixed to 700 mm while the wall thickness is not larger than 10 mm.

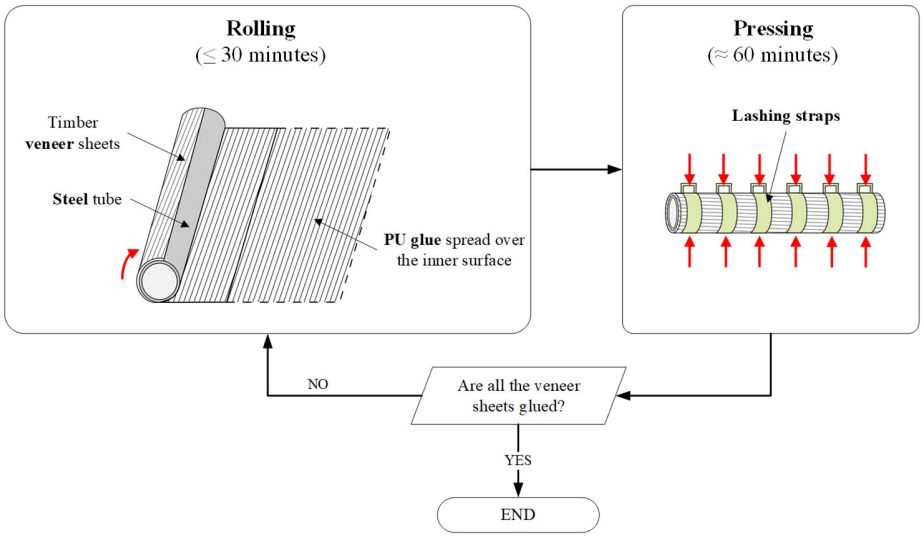

Figure 3: Schematic of the fabrication process of the "STIMBER-COL"

According to the fabrication process summarized in Figure 3, bi-component polyurethane (PU) glue has to be spread over the inner surface of the veneer sheets prior to rolling up, as in Figure 4. This glue requires a certain amount of water which has to be contained in the material itself in order to chemically react and ensure adequate adhesion. Hence, a certain humidity content shall be enforced in the veneer prior to gluing the veneer layers to the steel tube. For this purpose, the veneer sheets were placed in a storage room with a relative humidity of 40% and a temperature of approximately 21°.

Figure 4: Rolling-up of the 0.6 mm beech veneer sheets around the circular hollow profile.

As the single veneer sheets are 320 mm wide, some of them (e.g. 4-5) can be placed side by side and fixed along the edge through so-called "veneer tapes" to simultaneously wrap multiple sheets within the predefined open time (in this case ca. 30 minutes). Once the sheets are appropriately wrapped, the glue has to be adequately pressed over the entire surface for at least 60 minutes in order to ensure an effective bonding. Therefore, lashing straps can be adopted and tightened along the length to ensure uniform pressure. Finally, the process has to be iterated until the target wall thickness is reached. In addition, the veneer sheets could be slightly inclined by an angle ϕ with respect to the longitudinal direction to stabilize the tube along the circumferential direction. In this case, the layers are to be alternatively inclined by $+\phi$ and $-\phi$, respectively.

Finally, the resulting specimen can be further stored before testing in order to maintain the water content in the wood.

4.2. Test setup and loading

Based on preliminary analytical estimations of the maximum load, a test rig with a 1.6 MN hydraulic cylinder available in the laboratory of ETH Zürich was found to be the optimal solution for this experimental campaign. In order to capture all the non-linearities and the post-buckling behavior, the load is applied in displacement-controlled mode.

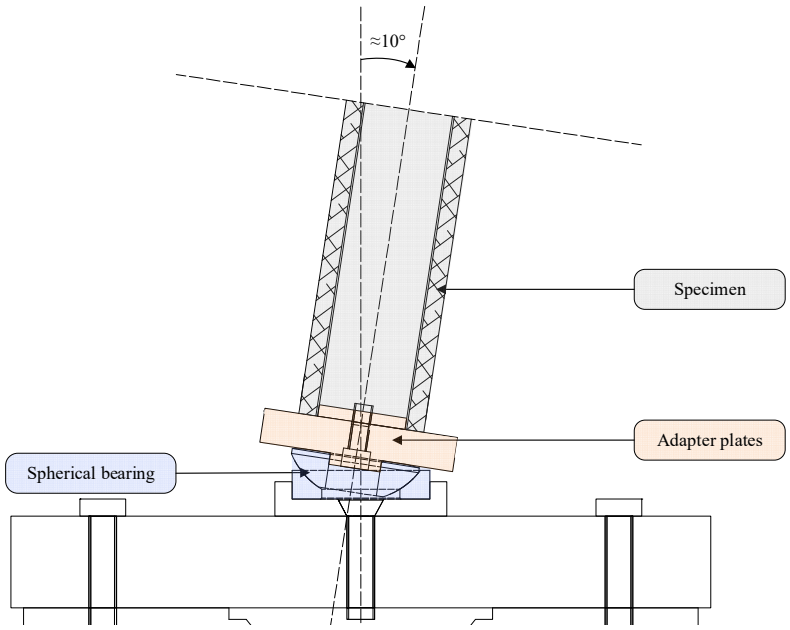

Figure 5: Detail of the base support of the test setup

4.3. Planning

As clarified in the previous sections, the objective of the experimental campaign is to assess the potential of the new steel-veneer column and to quantify benefit of the outer wrapped veneer layers on the static performance. Thus, in consideration of the preliminary nature of the study, the initially conceived 3 m long STIMBER-COL was downscaled to 2 m while the cross-sectional dimensions were proportionally adjusted. A total of 9 specimens is foreseen including 3 stub columns with a length of 300 mm which are meant to evaluate the cross-sectional plastic resistance without the occurrence of global buckling.

Two different wall thickness t_V of the veneer tube, with and without fiber inclination θ, will be investigated. Finally, to quantify the beneficial influence of the veneer-wrapping, the specimens are expected to be tested without veneer layers.

Table 1: Data of the test specimens

	STEEL		VENEER		GLOBAL
Specimen[1]	*D x t* (mm)	Grade (-)	t_v (mm)	θ (deg)	*L* (m)
S-80x1.5	80 x 1.5	S355	10.0	-	2.0
ST-80x1.5-0	80 x 1.5	S355	10.0	0	2.0
ST-80x1.5-15	80 x 1.5	S355	10.0	15.0	2.0
S-80x3	80 x 3.0	S355	10.0	-	2.0
ST-80x3-0	80 x 3.0	S355	10.0	0	2.0
ST-80x3-15	80 x 3.0	S355	10.0	15.0	2.0
S-80x1.5-B	80 x 1.5	S355	10.0	-	0.3
ST-80x1.5-0-B	80 x 1.5	S355	10.0	0	0.3
ST-80x1.5-15-B	80 x 1.5	S355	10.0	15.0	0.3

5. Numerical modelling

5.1. Mesh modelling, contact and boundary conditions

In addition to the experimental campaign described in the previous section, a numerical model was created to quantify the buckling resistance of the composite columns and to identify the key variables that affect the response. The numerical model was created through the software ABAQUS and it consists of a 3D non-linear finite element model using a combination of shell and solid elements to model the newly developed steel-veneer composite column.

4-node shell elements with reduced integration (S4R) were assigned to the inner steel hollow profiles and the outer veneer tube was modelled by means of three-dimensional 8-node elements (C3D8R). A reference mesh edge size of $\sqrt{0.5d \cdot t}$ was assumed by previous publications (Meng & Gardner, 2021). The columns considered in this numerical study refer to real-scale products of 3 m while all the geometrical and mechanical properties of the simulations will be provided in Section 5.5.

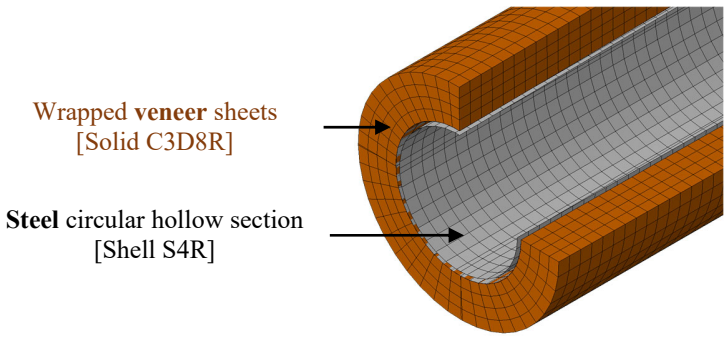

Figure 6: Assembly components of the finite element model of the STIMBER-COL

The connection between the steel tube and the inner surface of the first veneer layer is ensured by applying polyurethane glue. Accordingly, and given the nature of the specimen, no failure is expected to occur in the adhesive layer and both materials were fixed by means of a tie constraint in the numerical model.

The hinged ends of the columns, shown in Figure 5, were considered by coupling the extremities with a reference fixed point. All the translational degrees of freedom were restrained, except for the upper support where the vertical displacement was released.

5.2. Materials

The stress-strain relationship of steel was modelled by a linear-fully plastic relationship without hardening, where only the elastic properties (i.e. elastic modulus E_s and Poisson's ratio v) and the yield strength f_y of the material were required. The elastic modulus and Poisson's ratio were fixed at 210'000 MPa and 0.3, respectively, while the yield strength depends on the steel grade considered. However, more refined modelling may be implemented in future investigations based on the real material properties of the tested specimens.

Unlike structural steel, larger uncertainties are to be found in the material properties of timber veneer, as rather few experimental studies can be found in the literature. Given the orthotropic nature of the material, all the elastic and inelastic properties shall be defined for each of the three principal directions: longitudinal (parallel to the fiber), tangential (perpendicular to the fiber), radial (out-of-plane of the veneer layers). Buchelt and Wagenführ (2008) measured the main mechanical properties of beech veneer sheets, including the elastic modulus along the parallel (i.e. longitudinal) E_L and perpendicular direction (i.e. tangential) E_T of the fiber. Notwithstanding that the veneer thickness has a certain influence on the results, 0.5 mm thick beech veneer sheets exhibited a longitudinal and tangential elastic stiffness of 12'000 MPa and 630 MPa, respectively. These values were assumed in these studies while the elastic modulus along the radial direction E_R was taken as 630 MPa.

Experimental values of the shear modulus G can be found in (Staudacher, 2015), where a specimen made of a dozen of individual beech veneer thin sheets assembled with adhesive and subjected to bending. From these results, an average value of G_{LT} = 720 MPa (and assumed equal to G_{LR}) was obtained while a G_{TR} =100 MPa was taken (Quiquero, Gales, Abu, & Moss, 2018).

Due to the lack of measurements available, it is presumed that the Poisson's ratios along the three principal directions are similar to the values adopted for laminated veneer lumber (LVL).

The elastic properties for modelling the beech veneer used in this study are finally summarized in Table 2 and they are implemented by means of the feature *ENGINEERING CONSTANTS available in the section *ELASTIC of the material library.

Table 2: Assumed elastic properties of the veneer sheets

E_L (MPa)	E_T (MPa)	E_R (MPa)	v_{LT} (-)	v_{LR} (-)	v_{TR} (-)	G_{LT} (MPa)	G_{LR} (MPa)	G_{TR} (MPa)
12'000	630	630	0.55	0.55	0.2	720	720	100

The plastic linear-plastic stress-strain relationship is first given to define the uniaxial plastic and hardening behavior of the material and extended via an appropriate yield criterion. As typically shown in past numerical studies involving the use of timber and composite elements, there are several approaches and failure criteria which may be suitable for modelling timber veneer in structural applications. Notwithstanding that the classical Von Mises yield criterion presumes an isotropic plastic (i.e. plastic behavior is not dependent by the direction of the action), a more appropriate anisotropic plasticity model is necessary.

Among the numerous alternatives available in the scientific literature, two main yield criteria are to be mentioned, Hill's (1948) and Hoffmann's (1967) criteria. Whilst the former yield surface describes the plasticity/hardening of an orthotropic material, the more advanced Hoffmann's yield criterion differentiates between tension and compression response. These criteria as well as alternative and more advanced approaches were adopted and critically investigated in recent publications, as in the numerical study of Akter et al. (2021) where the timber specimens were subjected to combined compression and shear. As confirmed by these outcomes, Hill's criterion is more suitable for timber elements subjected to pure compression while the modelling of more complex load combinations could be better captured by more advanced approaches. These refined approaches require the implementation of complementary damage models accounting for the stiffness degradation in tension and shear (Xu, Bouchaïr, & Racher, 2014).

In view of the considerations on the modelling approaches available, because the veneer tube is expected to withstand mostly compressive stresses, Hill's criterion was deemed to be suitable for the application considered in this study. Although tension and shear may locally arise as a result of global and local instabilities, refined modelling methods may be included in the future upon measuring the actual material properties and evaluating the response of the whole specimens. It shall be noted that the differentiation of the failure between compression and tension would have required a FORTRAN subroutine to be implemented in the material definition (Eslami, Jayasinghe, & Waldmann, 2021).

Hill's criterion can be defined in ABAQUS by using the suboption *POTENTIAL in the module PLASTICITY. Owing to the associative nature of the criterion, the potential surface coincides with the yield. Surface. For this reason, the required input variables are the normal and shear strength along the principal directions, i.e. longitudinal, tangential and radial.

These unknowns were extrapolated by the experimental work of Buchelt and Wagenführ (2008) where tensile tests on 0.5 mm thick beech veneer were reported. From these results, the average values of 71.0 MPa and 7.9 MPa were used for the axial strength along the parallel f_L and perpendicular f_T direction. For the sake of simplicity, the strength along the radial direction f_R is kept equal to f_T. Although the aforementioned values refer to tensile strength, the yield compression and tensile stresses are the same according to the classic Hill's failure criterion. Thus, the values available were considered as axial strength irrespective of their sign, i.e. compression or tension. Similarly, the shear strength was taken as the measured average value of 11 MPa (Staudacher, 2015). The axial and shear strength values employed for defining the potential surface in the numerical model are finally provided below in Table 3.

Table 3: Axial and shear strength of the veneer sheets

$f_{t,L}$ (MPa)	$f_{t,T}$ (MPa)	$f_{t,R}$ (MPa)	$f_{v,LT}$ (MPa)	$f_{v,LR}$ (MPa)	$f_{v,TR}$ (MPa)
71.0	7.9	7.9*	11.0	11.0	11.0

It is worth noticing that no ultimate strain failure is given in this study as the main objective is to capture the main primary failure modes while the collapse of the columns at very high displacements can be evaluated more accurately at a later stage.

5.3. Fiber orientation of veneer

The different fiber orientation of the veneer layers was modelled via the feature MATERIAL ORIENTATION, enabling the user to define manually the principal directions of the material. Therefore, an appropriate cylindrical local coordinate system was first defined and the longitudinal direction was inclined by a given angle ϕ accordingly. As the veneer layers were overlapped by inclining the single elements in both directions alternately, the whole veneer tube was partitioned into two parts, see Figure 7(a), and the angles $+\phi$ and $-\phi$ were assigned, as shown in Figure 7(b) and Figure 7(c), respectively.

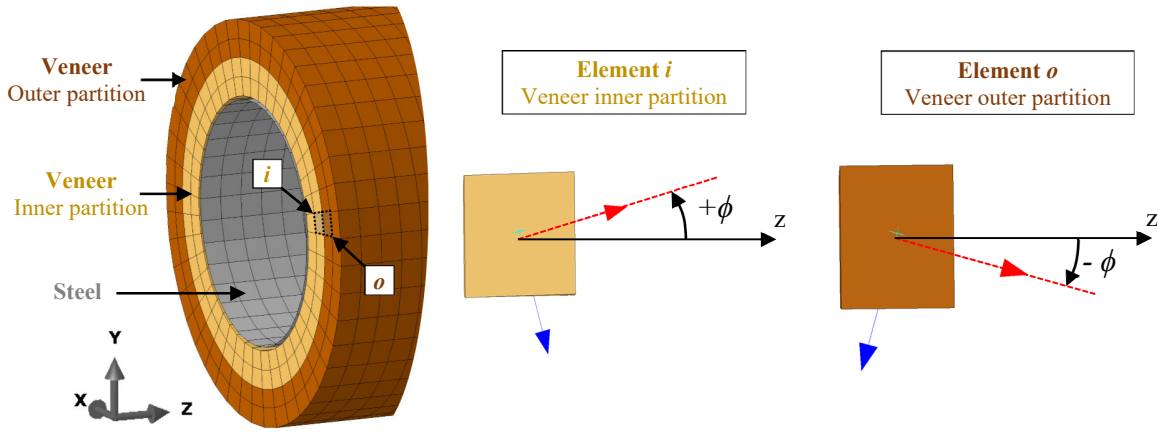

(a) (b) (c)

Figure 7: (a) Partitioned parts of the FE model including the material orientation of the (b) inner and (c) outer elements for modelling the fiber orientation of the veneer

5.4. Solving procedure

The resulting FE model described in the previous sections is subjected to numerical simulation by applying a monotonic vertical displacement onto the upper end. To account for the material and geometric non-linearities of the system, a Geometric and Material Non-linear Analysis with Imperfections (GMNIA) was conducted according to a 2-step solving procedure. The first step

consists in the extrapolation of the initial imperfections based on the first buckling mode. For this purpose, a linear-elastic buckling analysis was carried out and the respective buckling shape (half-sine wave) was amplified by the initial imperfection. In this case, an equivalent imperfection value e_0 accounting for the geometrical and material imperfections, i.e. residual stresses over the cross-section, was employed. The recommended value of e_0 is provided in the draft document prEN 1993-1-12 (2021) related to the FE-assisted design methods, and it can be calculated as follows:

$$e_0[\text{mm}] = \max\left(\frac{\alpha L}{150}, \frac{L}{1000}\right) \quad (1)$$

Where α is the imperfection factor according to EN 1993-1-1 (2004) and L is the buckling length of the column in mm. The second step is the non-linear analysis of the composite column where both geometrical and material nonlinearities are considered. Prior to starting the simulation, the predefined equivalent imperfections defined by the amplified half-sine buckling shape were imported into the native FE geometry. The whole solving procedure is displayed in the flow-chart in Figure 8.

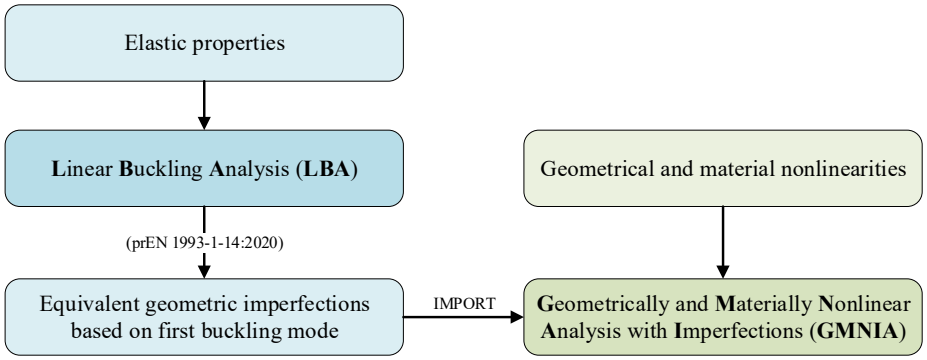

Figure 8: Flow-chart of the solving procedure used for carrying out the numerical simulations

5.5. Parametric study

The presented numerical model and solving procedure described in the previous section is utilized to investigate the global response of the new steel-veneer composite column in terms of resistance mechanisms and failure mode(s). In addition, a subset of geometrical and material variables falling within the expected field of application of the final product was selected and it is given in Table 4. All the possible combinations of input variables led to a total of 72 different configurations and 144 simulations (72 LBAs and 72 GMNIAs). The generation of the entire set of simulations as well as the post-processing of the output files were eased by ad-hoc Phyton scripts enabling the user to automatize the whole procedure.

Table 4: Variables of the parametric study

D (mm)	t (mm)	t_v (mm)	ϕ (deg)	f_v (MPa)	L (m)
80, 100	3, 4.5	10, 30, 50	0, 15, 30	460, 690	3.0

Where D and t are the outer diameter and the thickness of the steel profile, t_v is the thickness of the whole veneer tube, ϕ is the inclination angle of the fiber respect to the longitudinal direction, f_y is the nominal yield strength of steel and L indicates the height of the column.

The material properties of veneer were kept as indicated in Table 2 and Table 3 while the yielding strength values of steel given in Table 4 do not correspond to any characteristic values. However, as already mentioned, the objective of this parametric study lies in the qualitative evaluation of the main failure mode(s) and in the identification of the key variables and their influence on the global response of the composite column.

5.6. Discussion

Notwithstanding the high slenderness of the system, all the columns considered within the presented parametric study are expected to exhibit global flexural buckling, which was confirmed by the numerically obtained results.

From the evaluation of the load-(vertical) displacement curves, all the configurations share similar behavior, as shown in Figure 9: an initial linear-elastic branch up to the peak load as a result of global flexural buckling. The post-buckling stage is governed by a softening branch with a variable inclination.

To better comprehend the contribution of the steel and veneer tube throughout the simulation, the vertical load carried by the single material was plotted separately. With reference to Figure 9, the average (compressive) axial strain defined in Eq. 2 was considered to facilitate the interpretation of the results.

$$\bar{\varepsilon_z} = \frac{u_z}{A} \tag{2}$$

Where u_z is the vertical displacement applied at the upper end and A is the composite cross-section area.

Based on these plots, it can be seen that the peak load is related to the exploitation of the buckling resistance of the steel tube and the first plastic deformation can be observed at the mid-section. The composite action between the material at this stage can be considered negligible as no actual slip has occurred. For further vertical displacement, the buckling of the steel tube is restrained by the intact veneer layers resulting in a ductile response. However, as the deformation increases, the veneer undergoes crushing leading to a gradual reduction of the load-bearing capacity of the whole member. Finally, at large displacements, the external fibers of the veneer tube underwent local failure as a result of the buckling-induced bending moment.

It is worth noticing that the sequence of failure modes identified in the model is line with as the yield strain in steel is lower than the crushing strain of veneer. Thus, it could be argued that these values shall not significantly differ in order to ensure the exploitation of the strength of both materials.

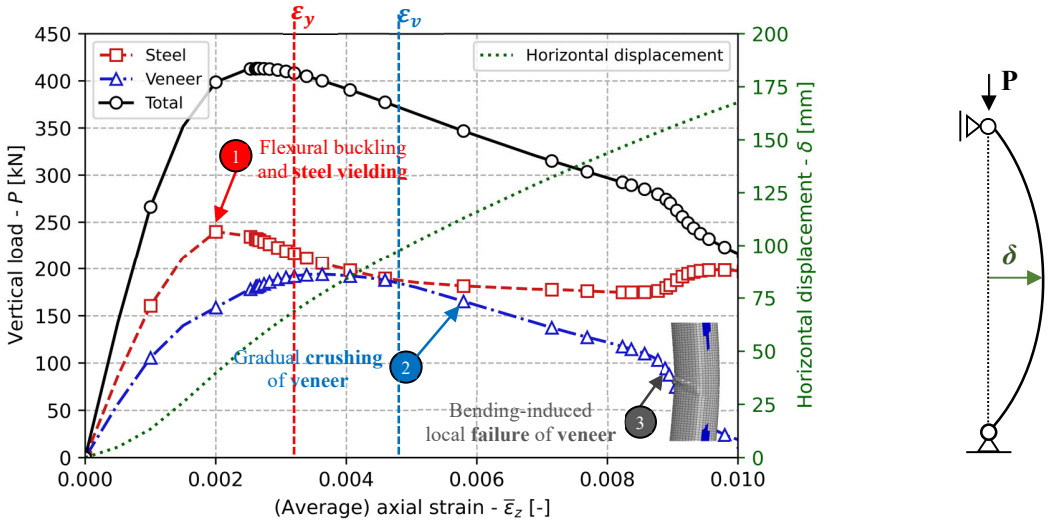

Figure 9: Vertical load-(average) axial strain curve including load components and horizontal displacement δ

From the evaluation of the load-strain curves of the simulations, the influence of the parameters on the response of the columns can be observed, see Figure 10. As the uncertainties of the material modelling represents an important factor, a qualitative assessment of the influence of key variables is presented in this section while a more detailed evaluation is foreseen in the next stages.

From the curves in Figure 10(a), it can be seen that the wall thickness of the outer veneer tube t_v enhances the cross-sectional and buckling resistance of the member thanks to the contribution by increasing the effective flexural stiffness. This leads to higher load while the post-buckling the post-peak softening branch seems steeper leading to an earlier failure of the outer veneer fibers. Conversely, the steel grade seems to have a beneficial influence on the buckling resistance and ductility, see Figure 10(b). Whilst the increase in resistance is justified by the higher yield strength, the better post-buckling response could be related to the cross-sectional strain distribution of both materials. In this regard, as already highlighted in recent studies (Kia & Valipour, 2021), the yield strain of steel and crushing strain of timber governs the activation of the ultimate resistance of both materials. In the case of S690 steel grade, the yield strain ε_y=3.3‰ and the crushing strain of veneer along the fiber $\varepsilon_{c,0}$=5.9‰ enable a subsequent activation of the veneer after reaching the yield strain in the inner steel tube at the peak-load. Lastly, as can be seen in Figure 10(c), the inclination of the veneer fiber shows a negative impact on the resistance due to the reduction in the flexural stiffness of the cross-section. However, a more beneficial effect of the fiber inclination was initially expected in the post-buckling range where the passive confinement of the veneer is activated. Nevertheless, more advanced material modelling and experimental results available in the near future could help address this issue while improving the accuracy of the FE model.

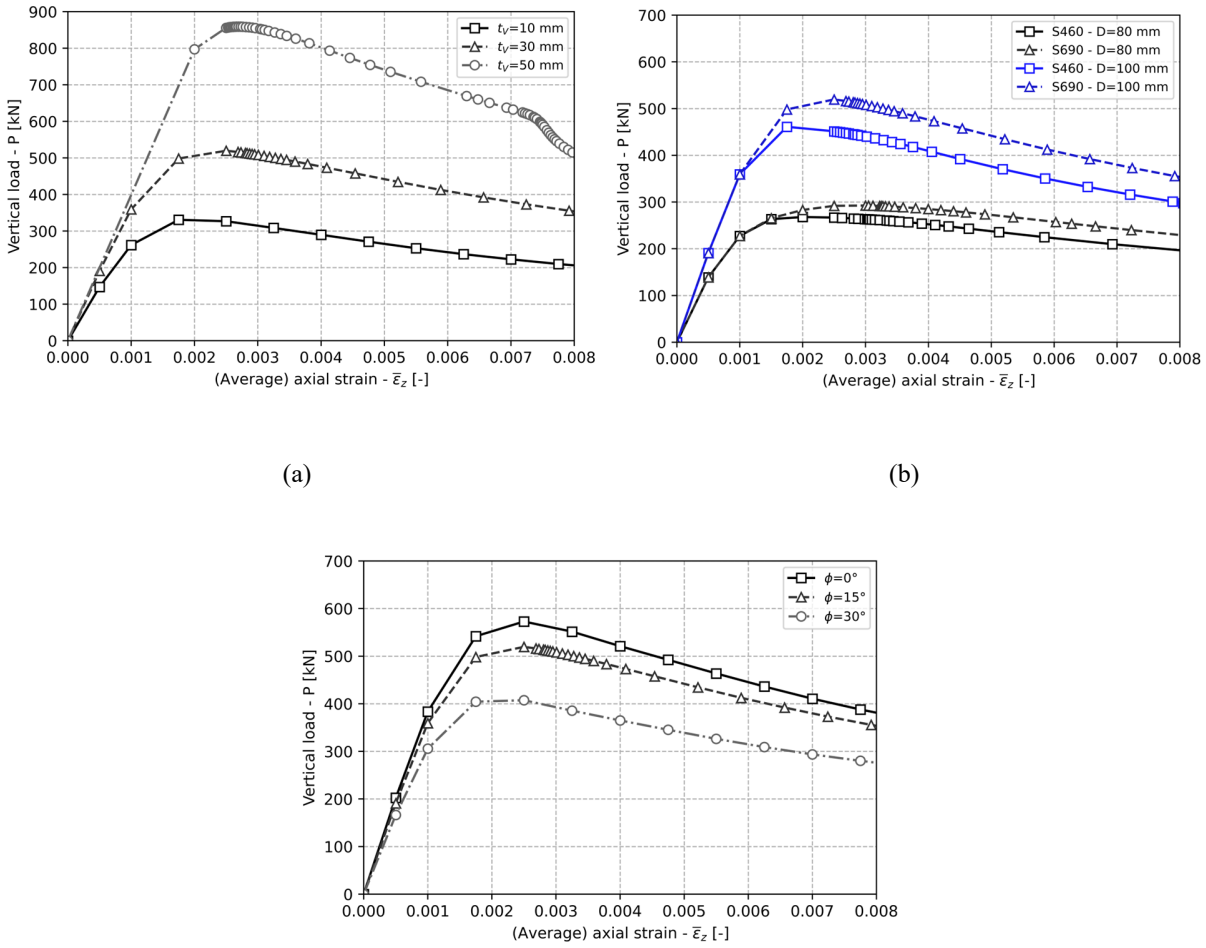

(a) (b)

(c)

Figure 10: Load-(average) axial strain for different parameters: (a) thickness of the veneer tube t_v, (b) steel grade and (c) inclination angle of the veneer fiber with respect to the longitudinal direction ϕ

5.7. Comparison with analytical predictions

To confirm the suitability of the parametric results in terms of maximum resistance, the peak load of the numerical simulations was finally compared with the analytical predictions. In the presented work, the buckling curves in EN 1993-1-1 (2004) accounting for the flexural buckling resistance has been taken in consideration as no local buckling effect seems to have negligible effect on the peak load. However, the formulation of the slenderness was to be adapted by including the flexural stiffness and the crushing resistance of the timber cross-section as follows:

$$\bar{\lambda} = \sqrt{\frac{f_y A_s + f_{c,\phi} A_{ve}}{N_{cr}(EI_{comp})}} \tag{3}$$

Where $f_{c,\phi}$ is the compressive strength of the veneer along the longitudinal direction with an angle ϕ with respect to the fiber direction, A_{ve} indicates the cross-sectional area of the veneer, and the composite flexural stiffness is given by:

$$EI_{comp} = E_s I_s + E_{v,\phi} I_v \tag{4}$$

Where $E_{v,\phi}$ is the elastic modulus of the veneer along the given direction whereas I_s and I_v are the second moment of area of the steel and veneer cross-section, respectively.

As the parametric study refers to steel cold-formed circular hollow sections (CHS), the buckling curve "c" was considered in accordance with the design provisions of EN 1993-1-1. The corresponding reduction factor χ accounting for flexural buckling was finally plotted and graphically compared with the numerically-derived values χ_{FE}. These were calculated backwards from the values of the maximum load as follows:

$$\chi_{FE} = \frac{N_{FE}}{f_y A_s + f_{c,\phi} A_{ve}} \tag{5}$$

Where N_{FE} is taken as the peak load reached in the numerical simulation.

From the results obtained and graphically summarized in Figure 11, it can be seen that the analytical relationships of EN 1993-1-1 lead to a seemingly conservative estimation of the buckling resistance of the composite steel-veneer columns investigated in the parametric study. The discrepancy becomes larger at larger wall thickness *tv*. Thus, it could be argued that the use of buckling curves for steel structures might not be sensibly extended to cover the composite steel-veneer columns investigated in this study and further investigations are required to determine appropriate modifications.

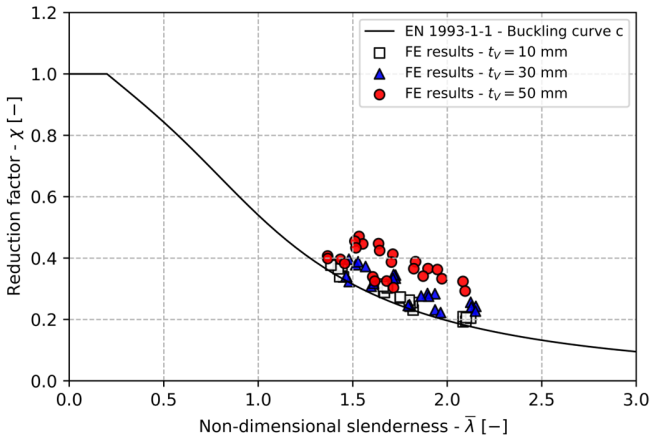

Figure 11: Reduction factors for flexural buckling from the parametric study and buckling curve of EN 1993-1-1.

6. Summary and outlook

The current work presents a newly conceived veneer-wrapped steel tubular columns "STIMBER-COL" with the support of foreseen experimental tests and a preliminary numerical study. Unlike more conventional composite solutions, a major challenge of the experimental study lies in the production of the specimens as single veneer sheets shall be adequately fixed to the inner steel tube and no scientific literature is available for such structural applications. Therefore, a step-by-step fabrication procedure was developed and it is described in this paper, including specimen production and curing. This method has been used for producing the specimens for being tested in the near future.

In parallel, a 3D non-linear finite element model of this composite column was developed with the software ABAQUS. This was used to conduct GMNIAs and a wide parametric study where the influence of some key variables was investigated. All the simulations followed a similar pattern where the axial resistance of the presented column "STIMBER-COL" is governed by flexural buckling as a result of the high slenderness of the columns considered. The post-buckling behavior is characterized by the yielding of the inner tube at mid-section while the bending-induced local buckling is delayed thanks to the confinement action of the undamaged outer veneer layers. Once the crushing strain of the outer veneer layer is reached, a drastic reduction of the capacity is observed leading to the failure of the column.

Whilst the numerical simulations showed promising results, the experimental results are essential to prove the potential of the given system, especially in terms of ductility. A first comparison between the numerical results and the adapted design rules of EN 1993-1-1 in terms of buckling resistance shows that the analytical prediction is conservative, especially for thick veneer tubes. Therefore, it could be argued that these rules may be further optimized for the product considered and alternative approaches available in the literature could be evaluated in future studies.

References

Akter, S. T., Serrano, E., & Bader, T. K. (2021). Numerical modelling of wood under combined loading of compression perpendicular to the grain and rolling shear. *Engineering Structures,, 244*, 112800.

British Standards Institution. (2004). *EN 1993-1-1:2004 Eurocode 3 - Design of steel structures Part 1-1: General rules and rules for buildings.*

British Standards Institution. (2021). *prEN 1993-1-14:2021 Eurocode 3 - Design of steel structures Part 1-14: Design assisted by finite element analysis.*

Buchelt, B., & Wagenführ, A. (2008). The mechanical behaviour of veneer subjected to bending and tensile load. *Holz als Roh- und Werkstoff, 66*, 289-294.

Djoubissie, D. D., Messan, A., Fournely, E., & Bouchaïr, A. (2018). Experimental study of the mechanical behavior of timber-concrete shear connections with threaded reinforcing bars. *Engineering Structures, 172*, 997-1010.

Eslami, H., Jayasinghe, L. B., & Waldmann, D. (2021). Nonlinear three-dimensional anisotropic material model for failure analysis of timber. *Engineering Failure Analysis, 130*, 105764.

Fragiacomo, L. (2013). Time-dependent behaviour of timber-concrete composite floors with prefabricated concrete slabs. *Engineering Structures, 52*(9), 687–96.

Ghanbari-Ghazijahani, T., Magsi, G. A., Gu, D., Nabati, A., & Ng, C. T. (2019). Double-skin concrete-timber-filled steel columns under compression. *Engineering Structures, 200*, 109537.

Hassanieh, A., Valipour, H. R., & Bradford, M. A. (2016). Experimental and numerical study of steel-timber composite (STC) beams. *Journal of Constructional Steel Research, 122*, 367-378.

Hill, R. (1948). A theory of the yielding and plastic flow of anisotropic metals. *Proceedings of the Royal Society of London*, *193 (1033)*, pp. 281-297. London.

Hoffman, O. (1967). The brittle strength of orthotropic materials. *Journal of Composite Materials, 1*(2), 200-206.

Hu, Q., Gao, Y., Meng, X., & Diao, Y. (2020). Axial compression of steel–timber composite column consisting of H-shaped steel and glulam. *Engineering Structures, 216*, 110561.

Karagiannis, V., Málaga-Chuquitaype, C., & Elghazouli, A. Y. (2017). Behaviour of hybrid timber beam-to-tubular steel column moment connections. *Engineering Structures, 131*, 243–263.

Karampour, H., Bourges, M., Gilbert, B. P., Bismire, A., Bailleres, H., & Guan, H. (2020). Compressive behaviour of novel timber-filled steel tubular (TFST) columns. *Construction and Building Materials, 238*, 117734.

Karimi, K., El-Dakhakhni, W. W., & Tait, M. J. (2011). Performance enhancement of steel columns using concrete-filled composite jackets. *Journal of Performance of Constructed Facilities, 25*(3), 189-201.

Karimi, K; Tait, M J; El-Dakhakhni, W. W. (2011). Testing and modeling of a novel FRP-encased steel–concrete composite column. *Composite Structures, 93*(5), 1463-1473.

Keipour, N., Valipour, H. R., & Bradford, M. A. (2018). Steel-timber composite beam-to-column joints: effect of connections between timber slabs. *Journal of Constructional Steel Research, 151*, 132-145.

Kia, L., & Valipour, H. R. (2021). Composite timber-steel encased columns subjected to concentric loading. *Engineering Structures, 232*(111825).

Liang, Q. Q., Uy, B., & Liew, J. R. (2006). Nonlinear analysis of concrete-filled thin-walled steel box columns with local buckling effects. *Journal of Constructional Steel Research, 62*(6), 581-591.

LIGNOTUBE. (2023). *LIGNOTUBE wood tubes - the new wood material for hollow profiles*. Retrieved from LIGNOTUBE website: https://lignotube.de/

Loss, C., Piazza, M., & Zandonini, R. (2016). Connections for steel–timber hybrid prefabricated buildings. Part I: Experimental tests. *Construction and Building Materials, 122*, 781-795.

Meng, X., & Gardner, L. (2021). Flexural buckling of normal and high strength steel CHS columns. *Structures, 34*, 4364-4375.

Oudjene, M., Meghlat, E. M., Ait-Aider, H., Lardeur, P., Khelifa, M., & Batoz, J. L. (2018). Finite element modelling of the nonlinear load-slip behaviour of full-scale timber-to-concrete composite T-shaped beams. *Composite Structures, 196*, 117–126.

Quiquero, H., Gales, J., Abu, A., & Moss, P. (2018). Finite Element Modelling of Post-Tensioned Timber Beams under Fire Conditions. *SFPE 12th International Conference: Fire Engineering Solutions for the Built Environment.* Hawaii.

Romero, A., Yang, J., Hanus, F., & Odenbreit, C. (2022). Numerical Investigation of Steel-LVL Timber Composite Beams. *ce/papers, 5*, 21-30.

Shan, B., Xiao, Y., Zhang, W. L., & Liu, B. (2017). Mechanical behavior of connections for glubamconcrete composite beams. *Construction and Building Materials, 143*, 158–168.

Staudacher, R. (2015). *Ausgewählte mechanische Eigenschaften von Furnier der Holzarten. Fichte, Birke und Buche.* Technische Universität Graz, Institut für Holzbau und Holztechnologie. Graz: Fachbereich .

Xu, B.-H., Bouchaïr, A., & Racher, P. (2014). Appropriate Wood Constitutive Law for Simulation of Nonlinear Behavior of Timber Joints. *Journal of Materials in Civil Engineering, 26*(6).

Zhu, W., H, Y., W, L., B, S., Z, L., & H, T. (2019). Experimental investigation on innovative connections for timber–concrete composite systems. *Construction and Building Materials, 207*, 345-356.